

Theoretical analysis for optomechanical all-optical transistor

Mengying HE, Shasha LIAO, Li LIU, Jianji DONG (✉)

Wuhan National Laboratory for Optoelectronics, Huazhong University of Science and Technology, Wuhan 430074, China

© Higher Education Press and Springer-Verlag Berlin Heidelberg 2016

Abstract In this paper, we propose an on-chip all optical transistor driven by optical gradient force. The transistor consists of a single micro-ring resonator, half of which is suspended from the substrate, and a bus waveguide. The free-standing arc is bent by optical gradient force generated when the control light is coupled into the ring. The output power of the probe light is tuned continuously as the transmission spectrum red-shift due to the displacement of the free-standing arc. The transistor shows three working regions known as cutoff region, amplified region and saturate region, and the characteristic curve is tunable by changing the wavelength of the control light. Potential applications of the all optical transistor include waveform regeneration and other optical computing.

Keywords silicon photonics, optical gradient force, optical transistor

1 Introduction

The excavation of the optics as a tool in computing is significant in modern optical research field [1]. Optical computing systems using optical interconnect technology can have high space-bandwidth and time-bandwidth products, hence, many independent channels could be exploited for demanding computations. There is no interference and crosstalk when optical signal propagates in parallel channels, so the bottleneck effect in electronic computer can be overcome by parallel processing the data and information. Moreover, optical interconnect technology can break through the data exchange rate between computer cluster system and improve the effective operation speed. To achieve optical computing successfully, it is necessary to substitute the existing electronic components with new photonic components. A transistor that operates with photons rather than electrons is often

heralded as the next core device in optical computing [2].

Early work was based on Kerr effect and Raman effect, mostly in fiber-loop mirrors [3]. Some methods employed active directional coupler [4], single molecules [5], one stored photon [6], and micro-rings [7]. Instead of electronic or thermal control, which has more complicated manufacturing technology, of particular interest there is a new method to realize optical transistor based on optical gradient force. Barely a few nano-newton, can actuate waveguide to move for about tens of nanometers, and that is enough to change the effective refractive index and other characteristics consequently [8]. Cai et al. made great efforts on nanoelectromechanical system (NEMS) optical switch [9] and optical cross connector [10] using optical gradient force. However, a chip-level optical transistor which possesses both switching and amplification functionality is of vital importance since it comes up with light controlling light, and reduces the production cycle. In recent years, silicon based photonic devices have been making themselves the first priority due to the merits of which include small size, high speed, low cost and good compatibility with traditional complementary metal-oxide-semiconductor (CMOS) techniques.

In this paper, we propose an on-chip all optical transistor driven by optical gradient force. A bus waveguide and a micro-ring resonator are inclusive in this system. In particular, there is a released region covering half of the micro-ring. We first study on the optical gradient force to realize the continuous modulation of the stable displacement of the free-standing arc. Secondly we figure out the characteristic curve of the optical transistor and illustrate the functionality of switching and amplification. Finally we put forward two methods to optimize the characteristic curve of this optical transistor and, in addition, discuss the response frequency of the optical transistor for the real usage.

2 Principle of optical transistor

The schematic of on-chip all optical transistor is shown in

Fig. 1(a). A micro-ring resonator and bus waveguide with silicon material are fabricated on the silicon oxide (SiO_2) substrate. Half of the micro-ring resonator is designed to suspend from the substrate and leave a vertical nano-air-gap between the free-standing arc and the substrate. We choose a high-power monochrome light as the control light whose wavelength (λ_c) is slightly red-shifted from a resonant wavelength of the micro-ring resonator. The control light is first coupled into the ring and then coupled with the dielectric substrate through evanescent waves, and the energy in ring resonator is large enough to generate a vertical optical gradient force (attractive force) between the free-standing arc and the dielectric substrate. We choose a low-power monochrome light as the probe light, whose wavelength (λ_p) is exactly aligned with another resonant wavelength of the micro-ring resonator, and the power is too low to introduce any force into the opto-mechanical system. Then we characterize the output power of the probe light as a function of the power of control light. When the power of control light is very weak, the energy inside the ring is not high enough to deform the free-standing arc, then the resonant frequency is not shifted. Therefore, the probe light is totally coupled into the ring resonator and the output power is null, analog to the cutoff region of electronic transistor.

When the power of the control light is increased to some extent, the energy inside the ring is high enough to generate effective optical gradient force, which starts to bend the free-standing arc toward the substrate. Thus the effective refractive index of the ring is increased. Consequently, the resonant wavelength is red-shifted as illustrated in Fig. 1(b). Then the probe light changes its transmission from null transmission to a high transmission, analog to the amplified region of electronic transistor.

When the power of control light is further increased to a high level, the transmission of probe light remains the high transmission although the resonant wavelength is still red shifted to some extent. As a result, the output power will be saturated, analog to the saturation region. The characteristic curve of the optical transistor, defined by the relationship between the input power of the control light and the output power of the probe light, includes three operation states, cutoff region, amplified region and saturation region, shown in Fig. 1(c). When the input signal is a sinusoidal waveform with different power level, the output waveform in these three region is shrank, amplified and erased respectively, so the optical transistor possesses both functions of switching and amplification. Such approach could be a meaningful solution for waveform regeneration and other optical computing.

3 Results and discussion

Figure 2(a) shows the cross section of the micro-ring with half suspended. Both the bus waveguide and the ring resonator have a width of 500 nm and height of 220 nm. The gap between the bus waveguide and the ring resonator is 250 nm. The radius of the ring resonator is 20 μm . The initial air gap between the free-standing arc and the substrate is $g_0 = 200$ nm. As soon as the high-power control light is coupled into the ring, the arc bends with a central displacement x , assisted by the optical gradient force. The air gap is changed to $g = g_0 - x$ as illustrated in Fig. 2(a). Consequently, the effective refractive index of the arc is increased and the resonant wavelength is red-shifted from λ_{r0} to $\lambda_r = \lambda_{r0} + \delta\lambda_r$, where $\delta\lambda_r$ is the shift of resonant wavelength. The effective refractive index n_{eff}

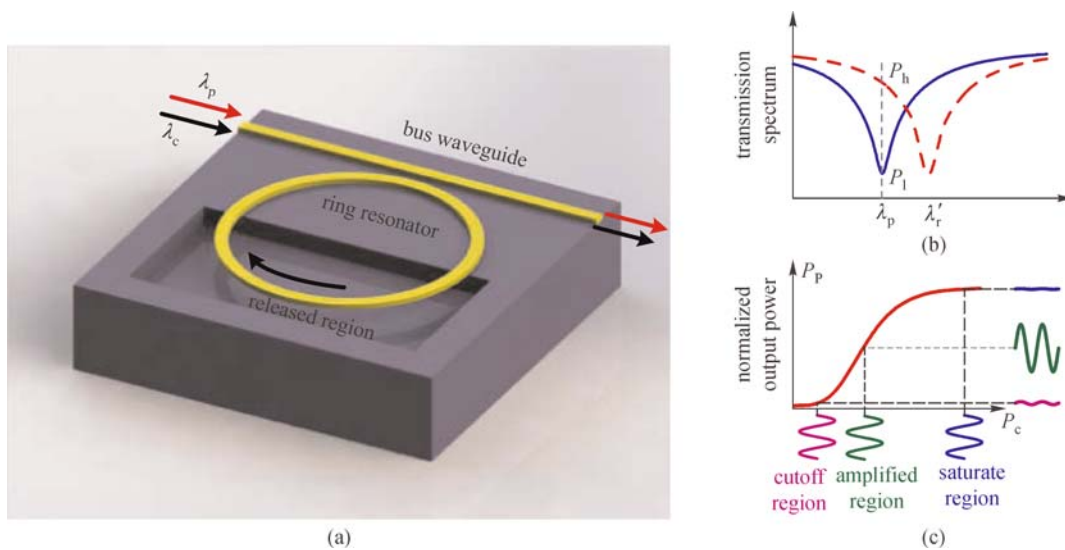


Fig. 1 (a) Schematic illustration of an all optical transistor driven by optical gradient force; (b) transmission spectra at a lower control power and red-shift at a higher control power; (c) illustration of the characteristic curve of the optical transistor which includes three parts: cutoff region, amplified region and saturate region

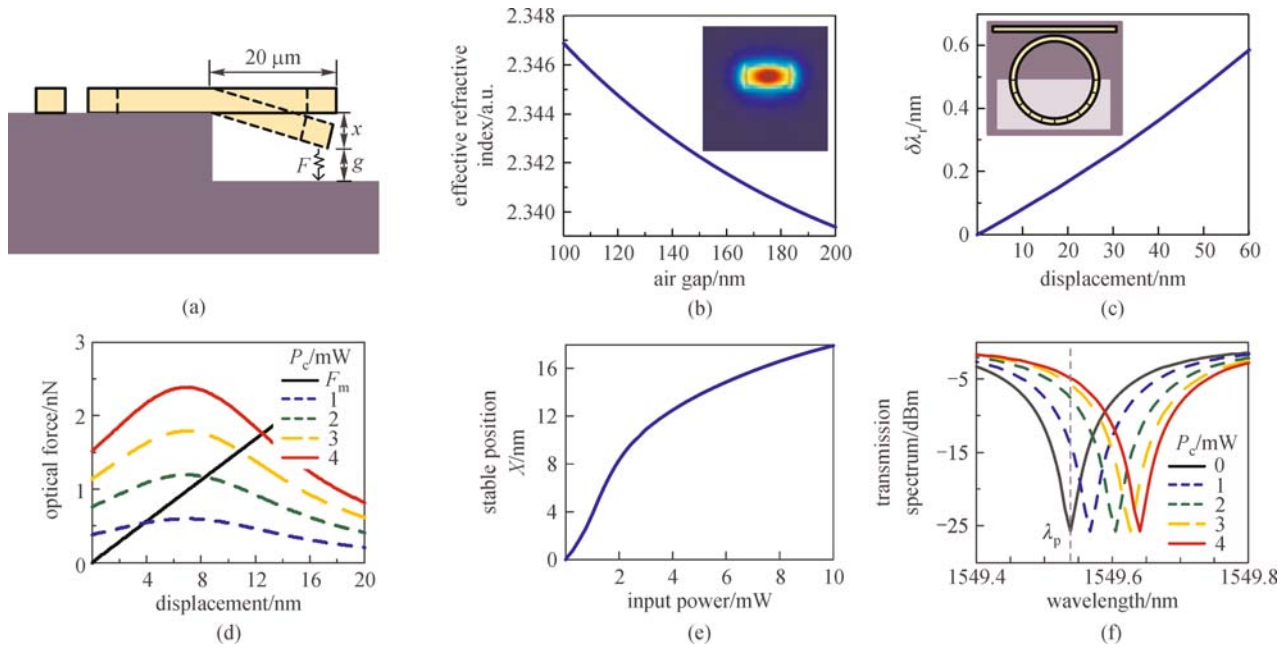


Fig. 2 (a) Illustration of the vertical optical gradient force; (b) simulation of the effective refractive index as a function of the air gap; (c) the shift of the resonant wavelength as a function of the displacement; (d) comparison of optical force and mechanical force under different power of the control light; (e) nonlinear relation between the displacement of the arc and the power of the control light; (f) transmission spectra of the ring resonator under different power of the control light

dependent to the air gap g can be solved using finite element method (COMSOL Multiphysics), which is shown in Fig. 2(b). To calculate the transmission spectrum and the resonant wavelength of the opto-mechanical micro-ring for various air gaps, we choose COMSOL Multiphysics with two dimension (2D) method. We first divide the arc into 10 parts evenly, and assign each of them an effective refractive index as if the arc is deformed and the displacement of each parts obeys the Euler-Bernoulli beam theory. Then the wavelength shift dependent on the displacement is shown in Fig. 2(c). The optical force can be expressed as [11]

$$F_{\text{opt}} = -\frac{1}{n_{\text{eff}}} \frac{\partial n_{\text{eff}}}{\partial g} U, \quad (1)$$

where the negative sign illustrate the direction of the optical force and U is the optical energy stored in the ring resonator, expressed as [12]

$$U = \frac{2\tau_e^{-1} P_{\text{in}}}{\left((\lambda_c - \lambda_r) 2\pi \lambda_r^{-2}\right)^2 + (\tau_i^{-1} + \tau_e^{-1})^2}, \quad (2)$$

where P_{in} is the power of the control light injected into the bus waveguide, λ_c is the wavelength of the control light, and λ_r is the resonant wavelength which is respected to the displacement of the suspended arc, τ_i^{-1} is the intrinsic decay rate due to the internal cavity loss and it is negligible, τ_e^{-1} is the extrinsic decay rate due to the externally coupling of the transmitted wave, it can be

calculate using the following expression [13]

$$\tau_e^{-1} = -\frac{\ln(1-k)C}{2\pi R n_{\text{eff}}}, \quad (3)$$

where k , R is the coupling coefficient and the radius of the ring resonator respectively, C is the speed of light in vacuum. In the case of $k = 0.05$, the extrinsic decay rate $\tau_e^{-1} = 5.20 \times 10^{10}$. Let us substitute Eq. (2) into Eq. (1), replace λ_r^{-2} with λ_{r0}^{-2} and remove τ_i^{-1} , the optical force is rewritten as

$$F_{\text{opt}} = -\frac{1}{n_{\text{eff}}} \frac{\partial n_{\text{eff}}}{\partial g} \frac{2\tau_e^{-1} P_{\text{in}}}{\left((\lambda_c - \lambda_r) 2\pi \lambda_{r0}^{-2}\right)^2 + \tau_e^{-2}}. \quad (4)$$

Subject to a control light of fixed wavelength and fixed power, the optical force is a nonlinear function of the central displacement of the arc, $F_{\text{opt}}(x)$.

Figure 2(d) shows a serial of nonlinear function for four different control powers at a fixed wavelength detuning, defined by the difference between the wavelength of the control light and the initial resonant wavelength of the ring resonator, $\Delta\lambda = \lambda_c - \lambda_{r0} = 0.05$ nm. As the displacement of the arc increases, the value of $\Delta\lambda$ decreases to zero then increases again, hence the amount of optical force reaches a maximum value when $\lambda_r(x) = \lambda_c$. Once the arc starts to deflect toward the substrate, the mechanical force (F_m) works at the same time and it is linear in the displacement x with a mechanical elastic coefficient $K_{\text{mech}} = 0.14$ N/m. The mechanical force as a function of the displacement is

shown as the black solid line. When the optical force dominates the mechanical force, the arc keep bending toward the substrate, on the contrary, the arc is pulled back until the two forces balanced each other at a intersect point of the two curves:

$$F_{\text{opt}}(x) + K_{\text{mech}}x = 0. \quad (5)$$

In Fig. 2(d), the four colorful lines represent optical force variation under different control powers, which is linearly increased from $P_c = 1$ mW to $P_c = 4$ mW, and the amount of optical force is positively correlative to the input power of control light. The intersect points with the line of mechanical force are $x = 3.83$ nm, $x = 8.3$ nm, $x = 10.9$ nm, $x = 12.53$ nm respectively. The optical force is less than the mechanical force in the right side of these intersect points and larger than the mechanical force in the left side, so these points are in a stable state of equilibrium and the arc can be oscillated or remain unchanged at this stable position, in other word, the solution of Eq. (5) represents the displacement of equilibrium, labeled as X . As the control power increases, the stable displacement is also increased, but the increment is gradually reduced. Figure 2(e) describes the displacement of equilibrium as a function of input power. We can see that, the stable displacement of the arc is continuously tuned by the power of the control light. Combined with the curve in Fig. 2(c) and in Fig. 2(e), we can figure out the transmission spectrum under any input control power. In Fig. 2(f), the transmission spectrum of the ring resonator under four different optical powers are illustrated. In the simulation, the Q factor of microring is 24596 and the notch depth is about -25 dB. The dark gray solid line is the initial transmission spectrum without any displacement of the free-standing arc. The value of the notch is chosen as the wavelength of the probe light, $\lambda_p = 1549.54$ nm. Hence the probe light is totally coupled into the micro-ring and there is no output power of the probe light. The input control power is linearly increased from $P_c = 1$ mW to $P_c = 4$ mW. The corresponding red-shift amounts of these resonant

wavelengths are $\delta\lambda_r = 0.0291$ nm, $\delta\lambda_r = 0.0661$ nm, $\delta\lambda_r = 0.0881$ nm, $\delta\lambda_r = 0.1019$ nm. As the transmission spectrum is red-shifted, the output power is increased fast first and slow gradually because of the trailing edge in the notch of the transmission spectrum. Based on the transmission spectra at different powers of control light, we can calculate the characteristic curve of optical transistor, as shown in Fig. 3(a). To optimize the characteristic curve, the wavelength detuning of control light, $\Delta\lambda = \lambda_c - \lambda_{r0}$, is very sensitive. When $\Delta\lambda = 0.05$ nm, we observe a preliminary character of transistor. The characteristic curve show a cutoff region and an amplified region, whose boundary is nearly $P_c = 0.75$ mW. However the saturation region does not appear. In other word, the boundary between the amplified region and the saturation region is inconspicuous. Moreover, the maximum normalized output power is about 0.4, which is far from the idea target.

We then simulate the transistor at another two cases, where $\Delta\lambda = 0.08$ nm and $\Delta\lambda = 0.10$ nm as shown in Fig. 3(a). When $\Delta\lambda$ is increased, the cutoff region is extended, the saturate region is gradually distinct and the maximum normalized output power is improved as well. All these good trends are attributed to the fast transition of equilibrium displacement. Figure 3(b) shows the stable displacement of the arc as a function of the input control power. When the input optical power is in a low level, the greater displacement is realized by small wavelength detuning, and when the input optical power is in a high level, the greater displacement is realized by large wavelength detuning. In fact, the characteristic curve in Fig. 3(a) results from a comprehensive behavior between the shift of transmission spectrum and stable displacement. Thus, the characteristic curve can be optimized by the amount of wavelength detuning, but there is a compromise since the Pull-Back Instability [12] will be induced to make the trace of the stable position of the arc more complicate when the wavelength detuning is large enough. To illustrate the performance of the optical transistor specifically, we assume the optical power of the control light is

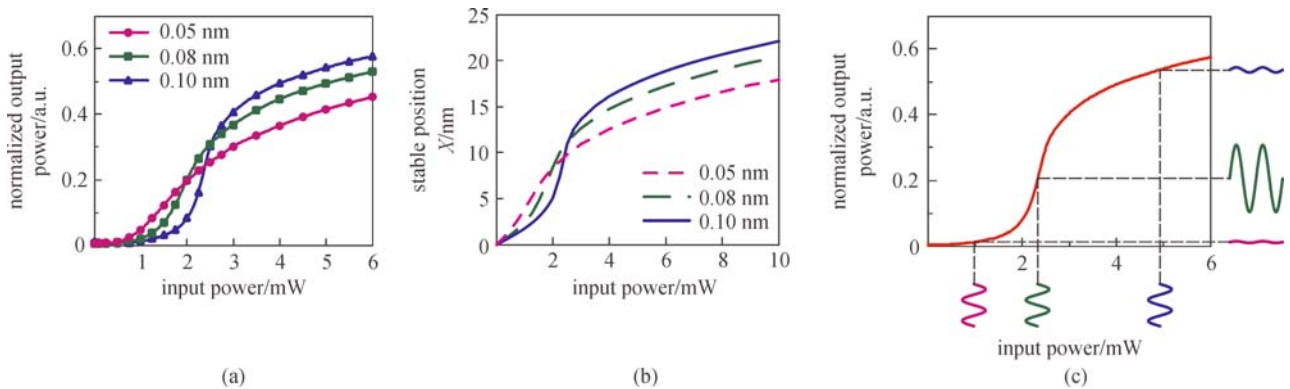


Fig. 3 (a) Relation between normalized output power and the input optical power of the control light under different wavelength detuning $\Delta\lambda$; (b) nonlinear relation between the displacement of the arc and the input optical power of the control light under different wavelength detuning $\Delta\lambda$; (c) illustration of the characteristic curve of the optical transistor while the wavelength detuning $\Delta\lambda = 0.1$ nm

time-varying, of which the waveform is a sinusoid. Figure 3(c) demonstrates the output waveforms of the probe light when the input control light lies in the different optical power levels. When the power level is in the cutoff region ($0 < P_c < 2$ mW), the output power is attenuated to null. When the power level is in the saturation region ($P_c > 3$ mW), the output optical power is up to the maximum but the magnitude of the sine waveform is diminished. When the power level is in the amplified region (2 mW $< P_c < 3$ mW), the magnitude of the waveform is amplified perfectly.

The characteristic curve is also very sensitive to the Q factor of the ring resonator, defined as the peak wavelength over bandwidth of full width at half maximum ($Q = \lambda_r / \lambda_{FWHM}$). The Q factor is related to the gap between the bus waveguide and the micro-ring. Figure 4(a) shows the transmission spectrum of the ring resonator under different gaps. When the gap is increased from 250 nm ($Q = 24596$) to 350 nm ($Q = 100622$), the notch of the transmission spectrum becomes deep and narrow. That means it is easier to reach the saturate region under the same shift of the resonant wavelength. The extrinsic decay rate is also strongly related to the gap because of the coupling coefficient k . Figure 4(b) shows the amount of the optical force dependent on the displacement at fixed wavelength detuning of 0.05 nm and fixed control power of 2 mW. We compare different microring with different gaps of 250, 300 and 350 nm. The extrinsic decay rate is $\tau_e^{-1} = 5.20 \times 10^{10}$, $\tau_e^{-1} = 3.61 \times 10^{10}$ and $\tau_e^{-1} = 2.36 \times 10^{10}$ respectively. As the extrinsic decay rate is reduced along with the enlarged gap, the curve of the optical force is shaper and the maximum value is bigger, the stable displacement of the arc is also increased. Hence enlarging the gap will change the nonlinear relation between the displacement of the arc and the power of the control light. Figure 4(c) shows the characteristic curve at different gaps. As the Q factor increases and gap becomes larger, the saturation region is gradually distinct and the maximum normalized output power is up to 100%, and the power boundary moves forward to about $P_s = 1$ mW.

For the practical employment of optical transistor, the response time is also very important. Actually, when we suddenly launch the control light to deform the photonic-mechanical ring resonator, it cannot reach the stable displacement immediately. It will oscillate and the oscillation will decay for a period of time. According to the Euler-Bernoulli beam theory, the lifetime τ can be expressed as [14]

$$\tau = \frac{2Ql^2}{\sqrt{\frac{Et^2}{12\rho}(\beta_n l)^2}}, \quad (6)$$

where $l = \pi R$ μm and $t = 500$ nm is the length and width of the free-standing arc respectively, $Q = 100$ is the quality of the free-standing arc, $\rho = 2330$ kg/m² stands for the mass density of the transistor material, $E = 169 \times 10^9$ N/m² is the Young's modulus. $(\beta_n l)$ obeys the equation that $\cos(\beta_n l) \cosh(\beta_n l) = 1$, n is the order of the mode. The solution are $\beta_1 l = 0.473$, $\beta_2 l = 7.853$, and $\beta_3 l = 10.996$. The response time will decrease quickly with the mode's order. So the first mode will make the most contribution to the vibration. In the case of fundamental vibration mode of the arc, the lifetime $\tau = 28.7$ μs , the respond frequency is 34.8 kHz. Therefore our optical transistor has a low frequency response, which may not be suitable for ultra-speed optical signal processing.

4 Conclusions

The on-chip all optical transistor driven by optical gradient force is demonstrated. The transistor consists of a single micro-ring resonator, half of which is suspended from the substrate, and a bus waveguide. The output power of the probe light is tuned continuously as the transmission spectrum red-shift due to the displacement of the free-standing arc. The transistor shows three working regions known as cutoff region, amplified region and saturate region, and the characteristic curve is tunable by changing

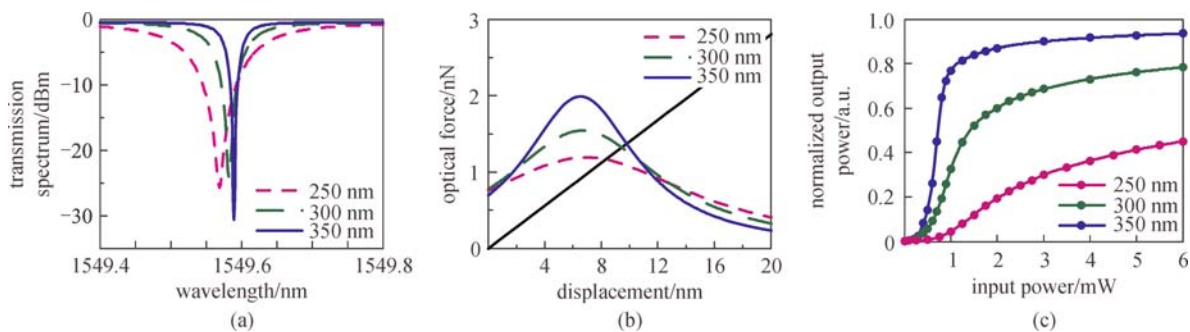


Fig. 4 (a) Transmission spectra of the ring resonator under different gaps; (b) comparison of optical force and mechanical force under different gaps while the power of the control light is 2 mW and the wavelength detuning $\Delta\lambda$ is 0.05 nm; (c) relation between normalized output power and the input optical power of the control light under different gaps

the wavelength of the control light. The characteristic curve is also optimized by analyzing the wavelength detuning, Q factor of micro-ring, and response frequency. Potential applications of the all optical transistor include waveform regeneration and other optical computing.

Acknowledgements This work was partially supported by the Program for New Century Excellent Talents in Ministry of Education of China (No. NCET-11-0168), and the National Natural Science Foundation of China (Grant Nos. 11174096 and 61475052).

References

1. Sawchuk A A, Strand T C. Digital optical computing. Proceedings of the IEEE, 1984, 72(7): 758–779
2. Miller D A B. Are optical transistors the logical next step? Nature Photonics, 2010, 4(1): 3–5
3. Starodumov A N, Barmenkov Y O, Martinez A, Torres I, Zenteno L A. Experimental demonstration of a Raman effect based optical transistor. Optics Letters, 1998, 23(5): 352–354
4. Krishnamurthy V, Chen Y, Ho S T. Photonic transistor design principles for switching gain ≥ 2 . Journal of Lightwave Technology, 2013, 31(13): 2086–2098
5. Hwang J, Pototschnig M, Lettow R, Zumofen G, Renn A, Götzinger S, Sandoghdar V. A single-molecule optical transistor. Nature, 2009, 460(7251): 76–80
6. Chen W, Beck K M, Bücker R, Gullans M, Lukin M D, Tanji-Suzuki H, Vuletić V. All-optical switch and transistor gated by one stored photon. Science, 2013, 341(6147): 768–770
7. Clader B D, Hendrickson S M. Microresonator-based all-optical transistor. Journal of the Optical Society of America B, Optical Physics, 2013, 30(5): 1329–1334
8. Povinelli M L, Loncar M, Ibanescu M, Smythe E J, Johnson S G, Capasso F, Joannopoulos J D. Evanescent-wave bonding between optical waveguides. Optics Letters, 2005, 30(22): 3042–3044
9. Cai H, Dong B, Tao J F, Ding L, Tsai J M, Lo G Q, Liu A Q, Kwong D L. A nanoelectromechanical systems optical switch driven by optical gradient force. Applied Physics Letters, 2013, 102(2): 023103
10. Cai H, Lin J X, Wu J H, Dong B, Gu Y D, Yang Z C, Jin Y F, Hao Y L, Kwong D L, Liu A Q. NEMS optical cross connect (OXC) driven by optical force. In: Proceedings of 28th IEEE International Conference on Micro Electro Mechanical Systems (MEMS), 2015
11. Pernice W H, Li M, Tang H X. Theoretical investigation of the transverse optical force between a silicon nanowire waveguide and a substrate. Optics Express, 2009, 17(3): 1806–1816
12. Ren M, Huang J, Cai H, Tsai J M, Zhou J, Liu Z, Suo Z, Liu A Q. Nano-optomechanical actuator and pull-back instability. ACS Nano, 2013, 7(2): 1676–1681
13. Little B E, Chu S T, Haus H A, Foresi J, Laine J P. Microring resonator channel dropping filters. Journal of Lightwave Technology, 1997, 15(6): 998–1005
14. Guo X, Zou C L, Ren X F, Sun F W, Guo G C. Broadband optomechanical phase shifter for photonic integrated circuits. Applied Physics Letters, 2012, 101(7): 071114



Jianji Dong is professor in Wuhan National Laboratory for Optoelectronics, Huazhong University of Science and Technology (HUST), Wuhan, China. He is working on the silicon photonics, photonic computing, and microwave photonics. He is an Editorial Board Member of *Scientific Reports*. He received the National Best Dissertations Award in 2010 and the first award of Natural Science of Hubei Province in 2013.